Time Evolution of Shear-Induced Structures in Semidilute Polystyrene Solutions

Takuji Kume,† Takayuki Hattori,‡ and Takeji Hashimoto*

Department of Polymer Chemistry, Graduate School of Engineering, Kyoto University, Kyoto 606-01, Japan

Received August 2, 1996; Revised Manuscript Received November 18, 1996[⊗]

ABSTRACT: We investigated time evolution of structures induced by imposing shear flow on semidilute solutions of high molecular weight polystyrene (PS) by means of both flow light scattering and rheology. PS with weight-average molecular weights of 5.48×10^6 and 2.89×10^6 were dissolved in dioctyl phthalate (DOP). After imposing shear flow with a shear rate $\dot{\gamma} > \dot{\gamma}_c$ (the critical shear rate for shear-induced concentration fluctuations), the unique butterfly-type scattering pattern appeared. The pattern had a scattering maximum along the flow direction. The wave number q_m and the intensity I_m at the scattering maximum decreased and increased, respectively, with time and eventually reached steady state values. The rheological experiments that were carried out on the same solution under the same shear flow revealed two stress overshoots. The second overshoot was found to be related to the development of butterfly pattern and its time change, i.e., to the formation and growth of shear-induced structures.

I. Introduction

Effects of flow on miscibility and structures in polymeric systems have attracted a great deal of attention in recent years. Even for studies concerning semidilute polymer solutions only, many experimental and theoretical studies have been carried out.[1−26] As far as our studies are concerned, we have been investigating the steady state behavior of semidilute solution of polystyrene (PS) with dioctyl phthalate (DOP) as a solvent (PS/DOP).[9,15,21,23,27] In this paper, we focus on a transient behavior of the PS/DOP systems, i.e., time evolution of the structure and stress developed after imposing simple shear flow to the solutions, as observed by flow light scattering and rheology.

For homogeneous semidilute solutions or melts in which polymer molecules are well entangled with each other, many rheological investigations have been reported. Stress developments in such systems after onset of shear flow have been studied minutely in the context of nonlinear viscoelasticity.[28−34] Upon imposing a high shear rate to such systems, a transient overshoot was observed in the shear and normal stress values. This phenomenon reflects the transient deformation of polymer chains and their subsequent relaxations within the "tubes", as proposed by Osaki et al.[30] and Doi-Edwards.[32]

In a recent rheological investigation, Magda et al.[35] reported the transient rheological properties in DOP solutions of high molecular weight PS. They showed that at a high shear rate the transient stress value exhibits two overshoots before reaching steady state. They suggested that the first and second overshoots are, respectively, due to chain stretching and shear-induced demixing. In this work we aimed to confirm the rheological behavior observed by Magda et al. for our samples and to directly investigate the transient structure formed under shear flow by using time-resolved light scattering.

Table 1. Polymer Solutions Used in This Work

polymer code	M_w[a] ($\times 10^{-6}$)	M_w/M_n[a]	concn (wt %)	c/c^* [b]	cloud point[c] (°C)	τ_R (s)[d]
PS548	5.48	1.15	3.0	20	16.3	5
PS548	5.48	1.15	6.0	40	13.8	50
PS288	2.89	1.09	8.0	40	12.8	140

[a] M_w and M_n are weight-average molecular weight and number-average molecular weight, respectively. [b] c^*: overlap concentration. [c] The cloud points of the solutions were determined by the same method as described elsewhere.[9] [d] The longest stress relaxation time measured from log η vs log $\dot{\gamma}$ at the experimental temperature specified in the text.

II. Experimental Method

II.A. Samples. The three polymer solutions used in this study consist of high molecular weight polystyrene (PS) dissolved in dioctyl phthalate (DOP). DOP is a θ solvent for PS, and its θ temperature (T_θ) is 22 °C.[36] Characterizations of the PS and their solutions are listed in Table 1. Concentrations of our solutions are in the semidilute regime. The methods used to prepare them are same as those used in previous experiments.[9,15,21,23,27]

The PS/DOP system has a phase diagram of the UCST-type. Figures 1 and 2 show, respectively, the cloud point curves of the PS548/DOP and the PS288/DOP systems used in this experiment. Crosses in the figures indicate the temperatures at which our experiments were carried out. Clearly all the samples are in one phase region in the quiescent state.

II.B. Shear−Light Scattering. Light-scattering measurements under shear flow (shear−light scattering) are carried out with the two rheo-optical apparatuses[23,37] constructed in our laboratory. One has a photodiode array as a one-dimensional detector for quantitative scattering measurements.[37] Another has a screen and CCD camera as shown in Figure 3. A He−Ne CW gas laser ($\lambda_0 = 632.8$ nm, 15 mW) is used as an incident beam source. The scattering pattern on the screen is captured by the CCD camera, and its NTSC video signal is transferred to a personal computer (Macintosh with frame grabber board), VCR, and so forth.[23] Although the scattering intensity data obtained by our CCD camera system are qualitative, the system enables us to take two-dimensional scattering profiles at short time intervals. The shear cell used is the same for both apparatuses, a transparent cone-and-plate type shear cell made of quartz with 80 mm diameter and 1° cone angle. The optical setup and coordinate system used in this study are the same as those previously used[27] and shown

* To whom correspondence should be addressed.
† Present address: Kao Corporation, Tokyo Research Laboratory, 1-3, Bunka 2-chome, Sumida-ku, Tokyo, 131 Japan.
‡ Present address: Sumitomo Rubber Industries, LTD., Research & Development H. Q., Innovative Technology Laboratory, 1-1, 2-chome, Tsutsui-cho, Chuo-ku, Kobe 651, Japan.
⊗ Abstract published in *Advance ACS Abstracts,* January 15, 1997.

S0024-9297(96)01167-9 CCC: $14.00

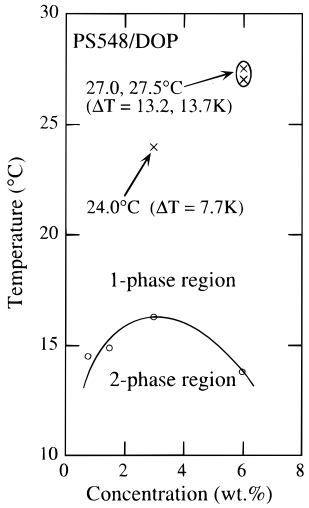

Figure 1. Cloud point curve of PS548/DOP. Crosses in the figure indicate the temperature and concentration at which experiments with shear−light scattering and rheometry were carried out.

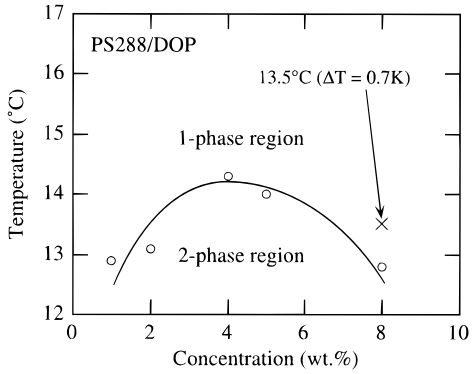

Figure 2. Cloud point curve of PS288/DOP. A cross in the figure indicates the temperature and concentration at which experiments with shear−light scattering and rheometry were carried out.

in Figure 3. The velocity gradient exists in the plane O_{xy}, where O_x is the flow direction. We send the incident beam along the Oy axis, and the scattering profiles were detected in the plane O_{xz}.

II.C. Temperature Control. The shear cell is covered by a temperature enclosure in both apparatuses in order to precisely control the sample temperature. The temperature enclosure has a double-chamber construction into which temperature-controlled air is fed, as shown in Figure 4. In the present experimental study, the sample temperature was controlled with accuracy of ±0.3 °C at the incident beam spot and within 1 °C variation along the radial direction. Before experiments we checked the temperature accuracy by using a specially made quartz plate in which three platinum resistance thermometers were embedded along the radical direction. The temperatures at the three points along the radial direction of the cone-and-plate shear cell filled with the DOP were measured by using the special plate. In order to make the temperature variation along the radial direction of the shear cell as small as possible, we used a metal pipe with holes for the metal shafts holding the cone and the plate, as shown in Figure 4. Through the holes the temperature-controlled air is circulated in the inner chamber and the pipe. Other temperature-controlled air is also circulated in the outer chamber. As shown in Figures 3 and 4, a window of the temperature enclosure for a scattered beam side has the shape of a truncated circle in the side of the shaft attached to the plate. Therefore scattering patterns are partially screened by the window, and their second and third quadrants on the detector plane are partially truncated (see the top view of the temperature enclosure in Figure 3) as seen in the patterns

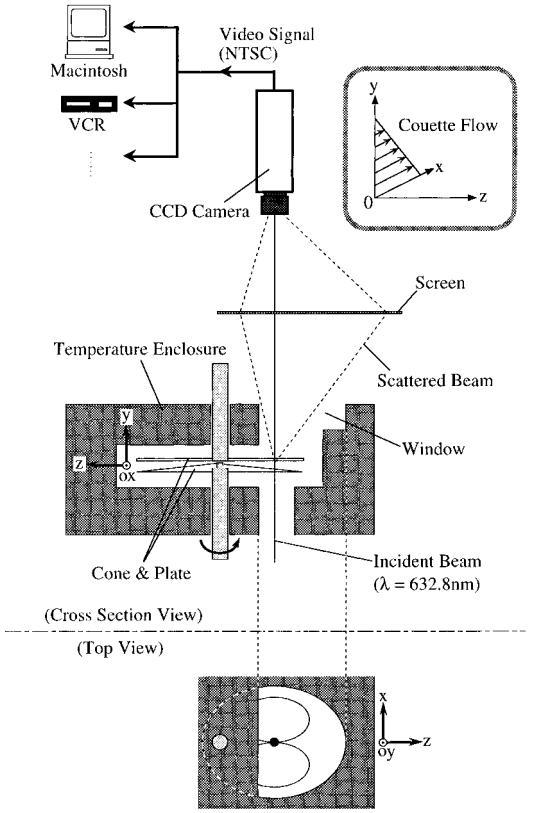

Figure 3. Schematic diagram of the experimental setup: CCD camera with image capturing system, temperature enclosure, cone-and-plate type shear cell to generate Couette flow, and coordinate system used in this study. Note that the coordinate system used here is identical to that commonly used in this field but is different from the one we used in our earlier work,[8,9,15,21,23] which is based on a tradition in the field of scattering. A top view of the temperature enclosure indicates that a window for the scattered beam side screens the butterfly pattern partially, causing asymmetrical appearance of the butterfly patterns in Figures 6, 8, 9, and 12.

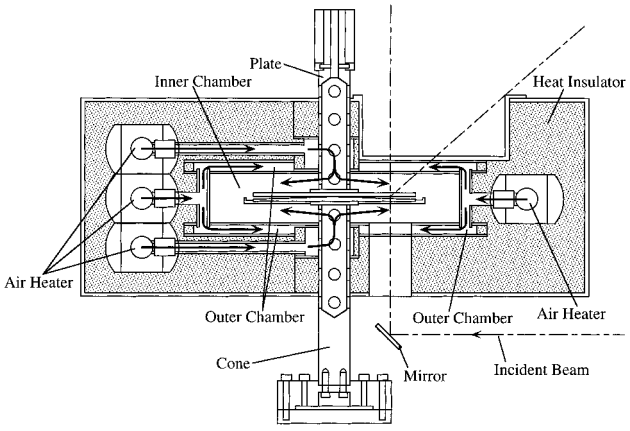

Figure 4. Cross-sectional view of the double chamber temperature enclosure. Solid arrows indicate flow of temperature-controlled air. The shafts holding the cone-and-plate are made out of a pipe with holes, through which the temperature-controlled air circulates in the inner chamber and the pipe. Other temperature-controlled air is also circulated in the outer chamber.

shown in Figures 6, 8, 9, and 12. For low-temperature experiments of PS288/DOP systems, we fed dried cold air to a temperature enclosure through an air-cooler set between the air compressor and the temperature enclosure.

II.D. Rheology. Rheological behavior was measured with a Rheometrics RMS800 mechanical spectrometer and RDA-II dynamic analyzer at almost the same temperature as in the

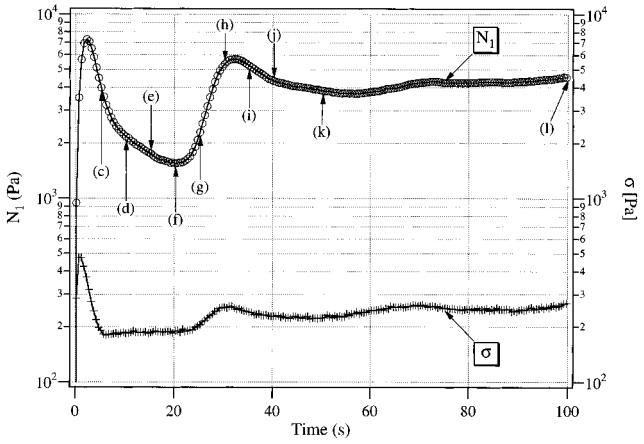

Figure 5. Plots of transient normal (N_1) and shear stresses (σ) of the PS548/DOP 6.0 wt % solution at 27.5 °C after the onset of the shear flow of $\dot{\gamma} = 14.3\ s^{-1}$.

shear-light scattering measurements. The rheological time τ_R (the longest stress relaxation time or the reptation time) was estimated for each solution used in this experiment (PS548/DOP 6.0 wt % at 27 °C, PS548/DOP 3.0 wt % at 25 °C, and PS288/DOP 8.0 wt % at 13.5 °C) from the shear rate $\dot{\gamma}_{c,rheo}$ at the intercept of two straight lines, one in the low-shear-rate Newtonian regime and the other in the high-shear-rate shear thinning regime, on a double logarithmic plot of steady state shear viscosity and shear rate ($\tau_R \equiv 1/\dot{\gamma}_{c,rheo}$). The results are summarized in Table 1.

III. Results

III.A. PS548/DOP Systems. Figure 5 shows the transient rheological properties of the PS548/DOP 6.0 wt % solution at 27.5 °C after the onset of shear flow of a constant shear rate $\dot{\gamma} = 14.3\ s^{-1}$. Both normal and shear stresses (N_1 and σ, respectively) showed two overshoots on its approach toward steady state. The second overshoot in normal stress is very conspicuous. These trends are completely the same as those reported by Magda et al.[35] The first overshoot in shear stress appears to occur prior to that in normal stress.

In order to investigate the structural origin of this intriguing rheological behavior, we carried out the two-dimensional scattering experiments using the shear−light scattering apparatus with CCD camera described in Figure 3, under almost the same conditions as that used for the rheological measurements in Figure 5. Figure 6 shows the time evolution of the scattering pattern after the onset of shear flow of $\dot{\gamma} = 14.3\ s^{-1}$ for the PS548/DOP 6.0 wt % solution at 27.0 °C. The flow direction (the O_x axis in Figure 3) is horizontal in the figure. Here, annotations (c)−(l) with arrows in Figure 5 correspond to those in Figure 6 and indicate the time when two-dimensional scattering patterns in Figure 6 were taken. In order to investigate in detail the development of scattering patterns after the onset of shear flow, we constructed contour patterns showing the iso-intensity levels for the scattering patterns. In the construction, we first smoothed the intensity fluctuations in the original scattering patterns which arise from the speckles in the patterns. Images (b)−(m) are the contour patterns obtained up to 150 s after the onset of shear flow. For comparison between the contour patterns and the original scattering patterns, we show real patterns (a) and (n) corresponding to contour patterns (b) and (m), respectively.

The scattering intensity along the flow started to increase at about 15 s (pattern (e)), and then the butterfly pattern was clearly developed: its intensity parallel to the flow direction increases and the "dark streak" perpendicular to flow direction narrows. The dark streak results from the fact that the scattered intensity normal to the flow direction stays weak, almost at the same intensity level as that in the homogeneous solutions. After 50 s (patterns (k)−(m)), the butterfly did not change much with time, which indicates achievement of a steady state.

To investigate the time evolution of the butterfly pattern more quantitatively, we evaluated the scattering profiles parallel to the flow direction (Figure 7). They are a part of the scattered intensity in the two-dimensional scattering patterns which falls onto the shaded area, as schematically illustrated in the inset at the top right-hand corner of Figure 7. The scattering intensity profiles shown are raw data subjected to no corrections, and hence these profiles are considered to be semiquantitative. The intensity at $q \leq 1.5 \times 10^{-4}$ nm^{-1} is very low, because a beam stop was set there. From right after the onset of shear flow (0 s) to 50 s, the scattered intensity increased by more than 1 order of magnitude, the scattering peak appeared, and its peak position moved to a smaller q with time. The scattering profile at 50 s was almost same as that of 100 s. Therefore the butterfly pattern reached a steady-state pattern after 50 s.

Figure 8 shows the plots of the transient normal (N_1) stress of the PS548/DOP 3.0 wt % solution at 24 °C after the onset of shear flow of $\dot{\gamma} = 89.1\ s^{-1}$. Note that the stress level developed here is much higher than that in Figure 5, because of a higher $\dot{\gamma}$ and a lower temperature than the corresponding values in Figure 5. Only the normal stress data were shown, because the second overshoot in normal stress was observed more clearly than that in shear stress. We also included the development of scattering patterns in terms of the contour patterns in Figure 8. These contour patterns were constructed in the same manner as in Figure 6 from the original scattering patterns taken at the time indicated by the arrow on the data line of normal stress. The shear rate of $89.1\ s^{-1}$ chosen is high enough that it belongs to regime IV[15,27] showing the anomalous rheological and scattering behavior (see Figure 2 of ref 27 for the same solution with the same concentration or Figure 11, shown later, for the same solution with a higher concentration). We will discuss later in section IV.A about the anomaly in regime IV. Because of the large $\dot{\gamma}$ ($89.1\ s^{-1}$) imposed to the system, the normal stress was so large that their values at the first and second overshoots could not be properly detected: they were saturated. At 3 s after imposing shear flow at which the first stress overshoot was observed, no strong scattering yet appeared and the intensity level was the same as that in the quiescent homogeneous solution. At around the time at which the second overshoot occurred, a butterfly-like anisotropic scattering pattern developed. Then the scattering intensity increased with a further elapse of time, and a streak-like pattern perpendicular to the flow direction appeared at ca. 50 s after the onset of the flow. At this shear rate ($89.1\ s^{-1}$) the steady state scattering pattern is a strong streaklike pattern developed perpendicular to the flow direction which is superposed on the butterfly pattern appeared at larger angles, as shown in the contour pattern at 100 s.[27] Comparison of the scattering patterns taken at a much later time (though not shown in Figure 8) revealed that this pattern at 100 s is the steady state pattern.

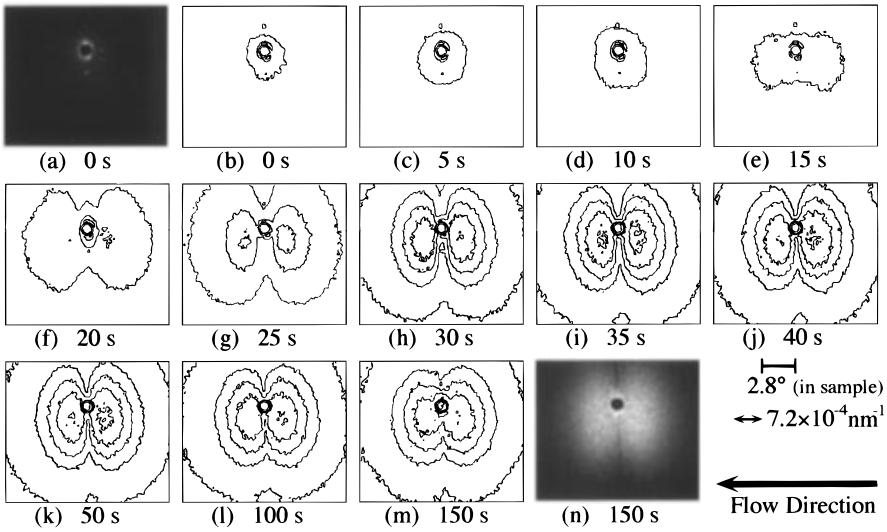

Figure 6. Time evolution of the scattering pattern of the PS548/DOP 6.0 wt % solution at 27 °C after the onset of the shear flow of $\dot{\gamma} = 14.3\ s^{-1}$. Images (a) and (n) are original scattering patterns, while others are contour plots of the scattered intensity distribution calculated from original scattering patterns. The asymmetry of the patterns with respect to the horizontal axis is due to an artifact induced by the window of the temperature enclosure as described in section II.B.

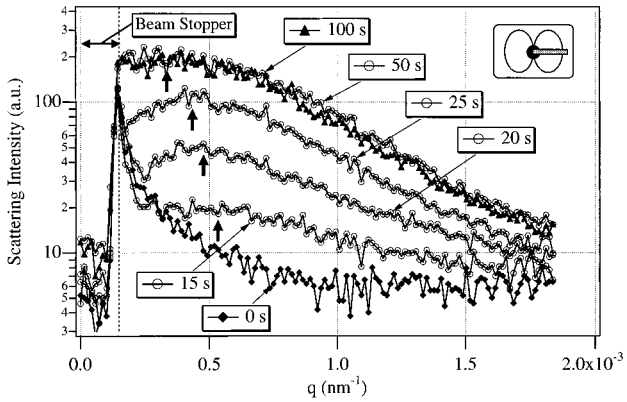

Figure 7. Time evolution of the scattering profiles along the flow direction which were calculated from the 2D scattering patterns shown in Figure 6.

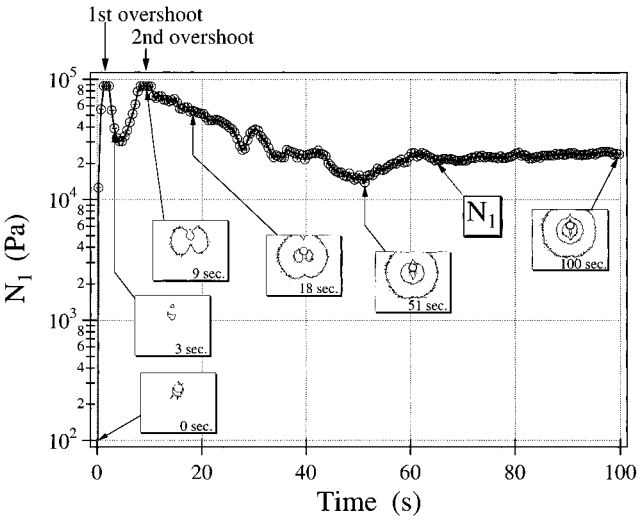

Figure 8. Time evolution of the scattering pattern and the normal stress (N_1) of the PS548/DOP 3.0 wt % solution at 24 °C after the onset of the shear flow of $\dot{\gamma} = 89.1\ s^{-1}$. This $\dot{\gamma}$ is much greater than $\dot{\gamma}_a$. The asymmetry in the contour patterns is for same reason as that in Figure 6.

III.B. PS288/DOP Systems. In order to investigate the time evolution of the butterfly pattern more quantitatively, we carried out the scattering and rheological experiments for the PS288/DOP 8.0 wt % solution at 13.5 °C ($\Delta T = +0.7$ °C, $\Delta T = T - T_{cl}$), i.e., at much lower temperature than those for the PS548/DOP systems, as shown in Figure 2. Because of small ΔT, the critical shear rate, $\dot{\gamma}_c$, for the butterfly formation is also very low.[9] Therefore, we could observe the phase-separation process under shear flow at a much lower shear rate than the previous cases shown in Figures 5−8. In the case of the lower shear rate, the time evolution of the scattering profile and the shear-induced structure formation are expected to occur more slowly, which facilitates a quantitative study on the shear-induced ordering processes.

Figure 9 qualitatively shows the time evolution of the butterfly pattern for the PS288/DOP 8.0 wt % solution at 13.5 °C after the onset of the flow of $\dot{\gamma} = 0.0144\ s^{-1}$, where the flow direction is horizontal. These scattering patterns were taken with photographic films. This development of the butterfly pattern is similar to that of PS548/DOP 6.0 wt % solution at 27 °C (Figure 6). However the shift of the peak position and the spreading of the butterfly wings with time can be more clearly observed in Figure 9.

For quantitative studies of the time evolution of scattering profiles, we used the shear−light scattering apparatus with a 35-element photodiode array as a one-dimensional detector. Using this apparatus we measured the time evolution of the scattering profiles parallel to the flow direction, which enabled us to quantitatively determine the time changes in the peak scattering vector q_m and the peak scattering intensity I_m parallel to flow. Figure 10a shows the time changes in q_m and I_m of the PS288/DOP 8.0 wt % solution at 13.5 °C after the onset of shear flow of $\dot{\gamma} = 0.0144\ s^{-1}$, the data of which were obtained simultaneously with the experiment shown in Figure 9. Figure 10b shows the results of transient rheological experiments on this sample under the same conditions as the scattering experiments. In this rheological experiment, the shear rate imposed ($0.0144\ s^{-1}$) was so low that the first normal stress was too small to be detected with sufficient accuracy. On the other hand, the shear stress (σ) could be accurately detected, showing the two overshoots as indicated by the arrows in Figure 10b.

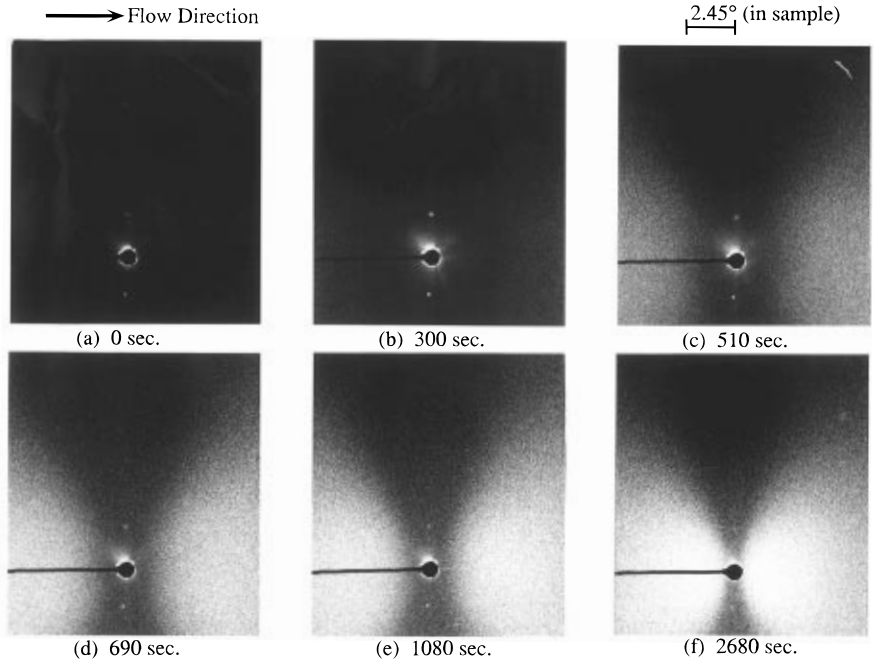

Figure 9. Time evolution of the scattering pattern of the PS288/DOP 8.0 wt % solution at 13.5 °C after the onset of the shear flow of $\dot{\gamma} = 0.0144\ s^{-1}$. These scattering patterns were taken by photographic films.

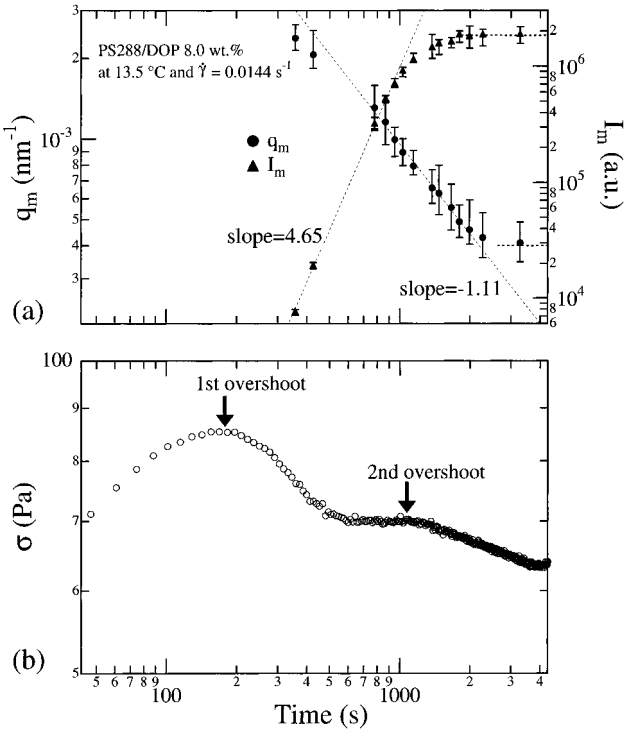

Figure 10. (a) Time changes in peak scattering vector q_m and peak scattering intensity I_m of the PS288/DOP 8.0 wt % solution at 13.5 °C after the onset of shear flow of $\dot{\gamma} = 0.0144\ s^{-1}$. The values q_m and I_m were quantitatively measured with a photodiode array detector. (b) Plot of transient shear stress (σ) of the same sample under the same conditions as in (a).

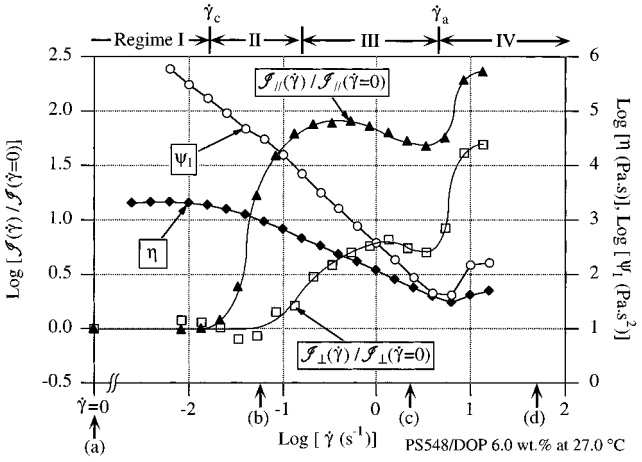

Figure 11. Shear viscosity, η, coefficient of the first normal stress difference, ψ_1, normalized integrated scattered intensity parallel and perpendicular to flow, $I_{\parallel}(\dot{\gamma})/I_{\parallel}(\dot{\gamma}=0)$ and $I_{\perp}(\dot{\gamma})/I_{\perp}(\dot{\gamma}=0)$ for the PS548/DOP 6.0 wt % solution in steady state shear flow at 27 °C. $\dot{\gamma}_c$ and $\dot{\gamma}_a$ are the critical shear rates for the onset of the shear-enhanced concentration fluctuations and of the anomalies in the rheological and scattering behavior, respectively.

IV. Discussion

IV.A. Steady State Structures and Properties as a Function of $\dot{\gamma}$. Before we discuss the transient structures and properties, it would be useful to briefly review steady state structures and properties.[15,21,27] Figure 11 shows the steady state scattering and rheological properties of the PS548/DOP 6.0 wt % solution at 27 °C as a function of shear rate. $I_{\parallel}(\dot{\gamma})/I_{\parallel}(\dot{\gamma}=0)$ and $I_{\perp}(\dot{\gamma})/I_{\perp}(\dot{\gamma}=0)$ are, respectively, the integrated scattered intensity at a given $\dot{\gamma}$, normalized with respect to the integrated intensity of the quiescent solution, parallel and perpendicular to the flow direction. The definition of integrated intensity was given in previous papers.[9,27] η and ψ_1 are the shear viscosity and the coefficient of the first normal stress difference, respectively. Figure 12 shows a characteristic change in the steady state scattering pattern with $\dot{\gamma}$, corresponding to the changes shown in Figure 11. Patterns (a)−(d) of Figure 12 were obtained at $\dot{\gamma}$ marked (a)−(d) in Figure 11, and the flow direction is horizontal. We previously reported the steady state structure and anisotropic concentration fluctuations, in the PS/DOP solutions under shear flow by a direct visualization with shear microscopy, i.e., by *in situ* observation with optical microscopy.[21,23] The observed changes in the light scattering patterns and real-space structures with $\dot{\gamma}$ were summarized in Figure 10 of ref 27.

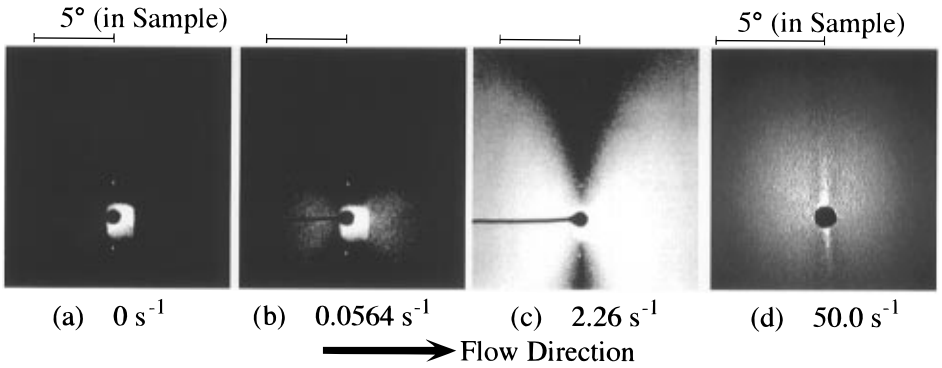

Figure 12. Steady state scattering patterns at various shear rates for the same solution as in Figure 11. Pattern d was taken with a shorter exposure time than the other patterns. The asymmetry of the LS patterns is due to the same origin as that in Figure 6.

The shear-rate dependence of the scattering and rheological behavior can be classified into four regimes, as shown in the top margin of Figure 11; regime I at $\dot{\gamma} < \dot{\gamma}_c$, where $\dot{\gamma}_c$ is the critical shear rate for the *shear-enhanced concentration fluctuations or phase separation*, and regimes II−IV at $\dot{\gamma} > \dot{\gamma}_c$. In regime I, the scattering and concentration fluctuations are essentially identical to those of homogeneous semidilute solutions, and rheological behavior is almost that of Newtonian fluid. In regime II, a unique butterfly-type scattering pattern appears with a dark streak perpendicular to the flow direction. The scattered intensity $I_{\parallel}$ is increased by about 2 orders of magnitude, but $I_{\perp}$ is still weak. In regime III, $I_{//}$ reaches nearly a steady value but $I_{\perp}$ still increases. Thus the butterfly pattern changes in such a way that its wings open and the dark streak narrows. In regimes II and III, η and ψ_1 decrease with increasing $\dot{\gamma}$, i.e., shear thinning occurs.

In regime IV (at $\dot{\gamma} > \dot{\gamma}_a$, where $\dot{\gamma}_a$ is the second critical shear rate or the critical shear rate for the onset of the anomalous behavior), the intensities $I_{\parallel}$ and $I_{\perp}$ further increase and the butterfly pattern changes into the two-point pattern elongated normal to the flow (the tendency being especially remarkable in PS548/DOP 6.0 wt %) with a broad intensity maximum along the flow. Then at much higher shear rate in regime IV, a strong bright streaklike pattern oriented perpendicular to the flow appears at small-angle regions as seen in Figure 12d. This streaklike pattern is superposed on the two-point pattern at large q regions. These anomalies in the change of the scattering pattern with $\dot{\gamma}$ are closely related to anomalies in rheological behavior: Both η and ψ_1 turn and begin to increase in regime IV. In a previous report[15] for the PS548/DOP 6.0 wt % solution, we stated that there is no anomaly in η even in regime IV (though there is a definite anomaly in ψ_1), because the first overshoot of shear stress decays to the level expected from the $\dot{\gamma}$-dependence of η in the lower $\dot{\gamma}$ regime, if the solution is kept under shear. However we found that this solution exhibits further the second overshoot on its approach toward steady state, if the solution is kept under shear even longer, and that the steady values are larger than those reported previously. Therefore this solution was found to exhibit the anomaly in both η and ψ_1, as shown in Figure 11 and a report Yanase et al.[12]

IV.B. Transient Behavior in PS548/DOP Systems. Figure 6 indicates that the butterfly pattern starts to grow at ca. 15 s after the onset of shear flow of $\dot{\gamma} = 14.3$ s^{-1} for the 6.0 wt % solution. Furthermore, from Figure 5 we find that this change occurred after the first stress overshoot and near the minimum in N_1 in the plot of log N_1 vs t. Further comparison of Figures 6 and 7 with Figure 5 shows that the butterfly pattern reached almost steady state after the second stress overshoot, i.e., at >50 s.

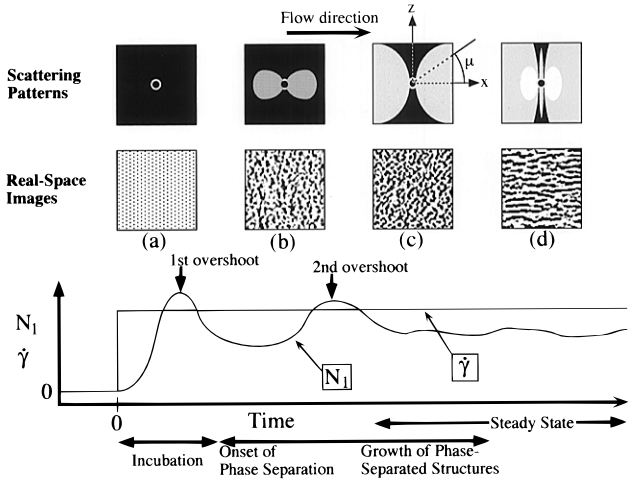

Figure 13. Schematic representation of transient changes in the butterfly-type light-scattering pattern, the microscope (real-space) image for the concentration fluctuations, and the normal stress after the onset of the flow at a constant shear rate $\dot{\gamma}$. The dark and bright regions in the microscope images correspond to polymer-rich and polymer-poor regions, respectively. The angle μ on the scattering pattern indicates azimuthal angle. Parts a and b represent the incubation state and the early stage of the shear-induced phase separation. In the case of a low imposed shear rate satisfying $\dot{\gamma}_c < \dot{\gamma} < \dot{\gamma}_a$, the steady state is represented by part c and the change from parts a and c corresponds to a growth of the phase-separated structures. In the case of a high imposed shear rate, the steady state is represented by part d, while the growth of the structures by the change from part b to c and finally to d.

The trends found above are schematically summarized in Figure 13 where the changes in the light-scattering patterns, the real-space structures, and the normal stress with time after the onset of a constant shear rate are schematically shown and classified into three regions. First, some incubation time exists from the onset of shear flow to evolution of the butterfly pattern for the q window covered in our light-scattering experiments (part a). Note that the structure development occurs at around a time at which N_1 becomes minimum after the first stress overshoot (part b). Furthermore the system reaches steady state after the second overshoot. The steady state scattering pattern and structures at this shear rate of $\dot{\gamma} = 14.3$ s^{-1} are shown in part c. Note that part d refers to the case in which the imposed shear rate $\dot{\gamma}$ is much higher than $\dot{\gamma}_a$ (e.g., 50.0 s^{-1} in Figure 12d). As the steady state is

approached (from (b) to (c) in Figure 13), the butterfly wings become wider, giving rise to a thinner dark streak normal to flow. The corresponding schematic real-space images, i.e., real structures of the sample under flow, are shown beneath the scattering patterns. The dark and bright regions correspond to polymer-rich and polymer-poor regions, respectively. Right after the onset of the evolution of the butterfly pattern, the wave vectors **k** for the Fourier modes of the shear-enhanced concentration fluctuations are spread over a narrow range of orientation angles around the flow direction; that is, the fluctuations are enhanced primarily only along flow. Therefore the scattering pattern spreads over a narrow azimuthal angle, μ, around $\mu = 0°$. As time elapses the wave vectors **k** spread over a wider angular range around the flow direction, and hence the butterfly wings become wider.

Figure 8 for the case of a high imposed shear rate of $\dot{\gamma} > \dot{\gamma}_a$ also indicates that the scattering pattern starts to grow after the first stress overshoot. In the beginning of the development of the scattering pattern, the shape of anisotropic scattering pattern is butterfly-type. However, the steady state scattering pattern is the strong streaklike pattern at small q regions superposed on the two-point pattern at large q regions. These developments of scattering patterns are very similar to those under steady shear flow with increasing $\dot{\gamma}$ as shown in Figure 10 of ref 27. The development of the transient scattering and structure at the high shear rate is also represented schematically by Figure 13. However, it should be noted that at this high shear rate the steady state scattering pattern and structures are given by part d instead of part c. Although the steady state is different, the time evolution is also classified into three regions, i.e., incubation, evolution, and steady state regions. The early stage of the structure development at the high shear rates ($\dot{\gamma} > \dot{\gamma}_a$) (whose steady state pattern and structure are given by Figure 13d) is same as that at the low shear rates ($\dot{\gamma}_c < \dot{\gamma} < \dot{\gamma}_a$) (whose steady state is given by Figure 13c). It occurs after the first stress overshoot and around a time at which the stress becomes minimum (part b). The structure growth and evolution of the butterfly patterns after the onset of the phase separation are shown in parts b and c. As shown in Figure 13d, however, the steady state structure has long strings aligned parallel to the flow (part d). It is believed that these strings themselves have internal concentration fluctuations along their axes. The strings give rise to the strong streaklike pattern at small q regions and the internal concentration fluctuations are responsible for the two point pattern at large q regions.[27]

IV.C. Transient Behavior in PS288/DOP Systems. Figures 9 and 10 indicate that the scattering intensity of the butterfly patterns started to increase after 300 s, shortly after the first overshoot at ca. 170 s (see arrow in Figure 10b). After that, log I_m increased and log q_m decreased almost linearly with increasing log t (see Figure 10a). This behavior in the time evolution of I_m and q_m suggests a slow ordering process of the structures in the solution after the onset of constant shear flow. This ordering process is very similar to that in spinodal decomposition in thermodynamically unstable solution without shear flow, except for the fact that the slopes in log I_m and log q_m versus log t are larger than those in the spinodal decomposition in quiescent solution. This result may strongly suggest that the butterfly patterns reflect the structure formation as a consequence of "shear-induced phase separation" rather than the shear-enhanced concentration fluctuations in single phase. The evolution of I_m and q_m stopped, and thus the system has reached the steady state at ca. 2000 s. During the phase separation and the structure-ordering process, the shear stress decays after the first overshoot and the second overshoot (see the arrow in Figure 10b) appears before the formation of the shear-induced steady state structures. The steady state is achieved, because structures above a certain size would be broken under shear flow and the broken structures tend to grow due to the shear-induced thermodynamic instability of the solutions.

IV.D. Comparison of the Transient Behavior in PS548/DOP and PS288/DOP Systems. The scattering and rheological behaviors in the PS288/DOP system is essentially same as those of the PS548/DOP system. However the transient behavior is more clearly resolved in the former than in the latter, because of the slower evolution of the structure and properties in the former. From the onset of shear flow to near the first overshoot, the scattering intensity was found to hardly increase with time; therefore the shear−flow-induced structures are not expected to be developed. Furthermore the strain value γ ($=\dot{\gamma}t$) at the maximum of the first overshoot in the PS288/DOP system (Figure 10b) is ca. 2.5. The corresponding strain values in the well-entangled homogeneous polymer solutions or polymer melts were reported to be typically in the range of 2-3.[28,32,34] Thus it is clear that the first overshoot is not necessarily due to the phase-separated structure. The origin of the first overshoot is probably the same as that encountered in normal, well-entangled homogeneous polymer solutions or melts subjected to large shear deformation and may be ascribed to the transient stretching of polymer chains and their relaxations within the tubes.[30,32]

The transient stretching of polymer chains may be more or less uniform, thus giving rise to no remarkable concentration fluctuations and hence scattering patterns. The overstretched chains tend to be relaxed through slippage of the entanglement couplings, which causes the decay of the first stress overshoot. This process is accompanied by the shear-induced concentration fluctuations due to the coupling of stress and the concentration fluctuations as postulated theoretically (the so-called elastic effect[5−7]) and as proposed experimentally (the so-called onset of the butterfly formation[3,9,11,12]). The concentration fluctuations further grow at a certain time after the onset of flow as shown in the changes in the butterfly patterns (Figures 6, 8, 9, and 13) and in the scattered intensity profiles parallel to flow (Figure 7). This structure growth may be responsible for the second overshoot. The overgrown structures will be burst by shear, but broken structures will grow due to the shear-induced thermodynamic instability of solutions. The burst and growth eventually give rise to steady state structures and stress. However an initial growth−burst process may give rise to a big effect on rheological properties, resulting in the observed second overshoots in shear and normal stresses.

IV.E. Comparisons with Earlier Reports. In this work we confirmed the postulate proposed by the rheological studies of Magda et al.[35] directly by means of the shear−light-scattering studies. Thus we conclude that first and second overshoots are due to the chain stretching followed by relaxation and the shear-induced demixing, respectively.

We very recently came across the report by Migler et al.[26] which was concerned with the transient rheology and shear−light-scattering experiments very similar to ours. They observed a very weak second overshoot in shear stress only at the highest shear rate ($\dot{\gamma} = 120\ s^{-1}$) employed in their experiment. The overshoot is so weak that a minimum of shear stress is only weakly discernible at ca. 8 s (see Figure 2a[26]). The weak overshoot is due to low molecular weight of PS ($MW = 1.03 \times 10^6$) and low concentration (4 wt % DOP solution) compared with our experiment. Though in our case the scattered intensity increased continuously with time as shown in Figures 7 and 10a, they found that the intensity at particular scattering vector gave an overshoot at ca. 8 s for $\dot{\gamma} = 120\ s^{-1}$ (see Figure 7a and Table 1).[26] The difference may be attributed to that in the plane of light scattering observation, i.e., *xz* (the velocity−neutral axis) plane in our case and *xy* (the velocity−velocity gradient) in their case. The fact that the scattered intensity becomes strong at the minimum in the shear stress vs time may be consistent with our result. Our conclusion about the origin of the first and second overshoots agrees with theirs.

V. Summaries

We can classify the time evolution of the butterfly pattern and the concentration fluctuations or phase-separated structures in the sheared solutions into three time regions. There is an incubation time between the onset of shear flow and the development of the butterfly pattern. During this incubation period, the first stress overshoot was observed, probably due to the instantaneous, more or less uniform deformation of entangled polymer chains and their relaxations within the tubes as proposed by Osaki et al.[30] and Doi-Edwards.[32] In our system the relaxations involve enhanced concentration fluctuations. Therefore the first overshoot ends with the onset of the butterfly pattern: the butterfly pattern appears at about the time when the stress reaches a minimum value after the first stress overshoot. It changes with time due to a further growth of concentration fluctuations or the shear-induced structures. This structure growth is responsible for the second stress overshoot. Finally the system attains the shear-rate dependent steady state structures after the second overshoot, due to a dynamical equilibrium between the growth of the structures driven by the shear-induced instability of the system and the burst of the overgrown structures driven by shear.

The first overshoot in our system is probably associated with the same mechanism as that proposed by Osaki et al. and Doi-Edwards for homogeneous semidilute polymer solutions or polymer melts subjected to a large deformation. The second overshoot in our system is confirmed to be due to growth of the phase-separated structures, before reaching shear-rate dependent steady state structures.

Acknowledgment. The authors are grateful to K. Matsuzaka for valuable discussions and technical help in the rheological experiments. This work was supported in part by a Grant-in-aid for Scientific Research on Priority Areas “Cooperative Phenomena in Complex Fluids” (07236103) addressed to T.H. and by a Grant-in-aid for Encouragement of Young Scientists-A (00062753) addressed to T.K., both from the Ministry of Education, Science and Culture, Japan.

References and Notes

(1) *ACS Symposium Series 597, Flow-Induced Structure in Polymers*; Nakatani, A. I., Dadmun, M. D., Eds.; American Chemical Society: Washington, DC, 1995.

(2) Ver Strate, G.; Philippoff, W. J. *J. Polym. Sci., Polym. Lett. Ed.* **1974**, *12*, 267.

(3) Wolf, B. A. *Makromol. Chem., Rapid Commun.* **1980**, *1*, 231.

(4) Rangel-Nafaile, C.; Metzner, A. B.; Wissbrun, K. F. *Macromolecules* **1984**, *17*, 1187.

(5) Helfand, E.; Fredrickson, G. H. *Phys. Rev. Lett.* **1989**, *62*, 2468.

(6) Onuki, A. *Phys. Rev. Lett.* **1989**, *62*,, 2472.

(7) Onuki, A. *J. Phys. Soc. Jpn.* **1990**, *59*, 3427.

(8) Hashimoto, T.; Takebe, T.; Fujioka, K. In *Dynamics and Patterns in Complex Fluids*; Onuki, A., Kawasaki, K., Eds.; Springer: Heidelberg, 1990; p 86.

(9) Hashimoto, T.; Fujioka, K. *J. Phys. Soc. Jpn.* **1991**, *60*, 356.

(10) Milner, S. T. *Phys. Rev. Lett.* **1991**, *66*, 1477.

(11) Wu, X.-L.; Pine, D. J.; Dixon, P. K. *Phys. Rev. Lett.* **1991**, *66*, 2408.

(12) Yanase, H.; Moldenaers, P.; Mewis, J.; Abetz, V.; van Egmond, J.; Fuller, G. G. *Rheol. Acta* **1991**, *30*.

(13) Larson, R. G. *Rheol. Acta* **1992**, *31*, 497.

(14) Doi, M.; Onuki, A. *J. Phys. II Fr.* **1992**, *2*, 1631.

(15) Hashimoto, T.; Kume, T. *J. Phys. Soc. Jpn.* **1992**, *61*, 1839.

(16) Dixon, P. K.; Pine, D. J.; Wu, X.-L. *Phys. Rev. Lett.* **1992**, *68*, 2239.

(17) van Egmond, J. W.; Werner, D. E.; Fuller, G. G. *J. Chem. Phys.* **1992**, *96*, 7742.

(18) Mavrantzas, V. G.; Beris, A. N. *Phys. Rev. Lett.* **1992**, *69*, 273.

(19) Moldenaers, P.; Yanase, H.; Mewis, J.; Fuller, G. G.; Lee, C.-S.; Magda, J. J. *Rheol. Acta* **1993**, *32*, 1.

(20) van Egmond, J. W.; Fuller, G. G. *Macromolecules* **1993**, *26*, 7182.

(21) Moses, E.; Kume, T.; Hashimoto, T. *Phys. Rev. Lett.* **1994**, *72*, 2037.

(22) Boué, F.; Lindner, P. *Europhys. Lett.* **1994**, *25*, 421.

(23) Kume, T.; Asakawa, K.; Moses, E.; Matsuzaka, K.; Hashimoto, T. *Acta Polym.* **1995**, *46*, 79.

(24) Hashimoto, T.; Matsuzaka, K.; Moses, E.; Onuki, A. *Phys. Rev. Lett.* **1995**, *74*, 126.

(25) Murase, H.; Kume, T.; Hashimoto, T.; Ohta, Y.; Mizukami, T. *Macromolecules* **1995**, *28*, 7724.

(26) Migler, K.; Liu, C.; Pine, D. J. *Macromolecules* **1996**, *29*, 1422.

(27) Kume, T.; Hashimoto, T. In *Flow-Induced Structure in Polymers*; Nakatani, A. I., Dadmun, M. D., Eds.; American Chemical Society: Washington, DC, 1995; p 35.

(28) Graessley, W. W. *Advances in Polymer Science, Vol. 16, The Entanglement Concept in Polymer Rheology*; Springer-Verlag: New York, 1974.

(29) Ferry, J. D. *Viscoelastic Proreties of Polymers*, 3rd ed.; Wiley: New York, 1980.

(30) Osaki, K.; Ohta, S.; Fukuda, M.; Kurata, M. *J. Polym. Sci.: Polym. Phys. Ed.* **1976**, *14*, 1701.

(31) Isono, Y.; Nagasawa, M. *Macromolecules* **1980**, *13*, 862.

(32) Doi, M.; Edwards, S. F. *The Theory of Polymer Dynamics*; Oxford University Press: Oxford, 1986.

(33) Takahashi, Y.; Isono, Y.; Noda, I.; Nagasawa, M. *Macromolecules* **1986**, *19*, 1217.

(34) Larson, R. G. *Constitutive Equations for Polymer Melts and Solutions*; Butterworths: Boston, 1988.

(35) Magda, J. J.; Lee, C. S.; Muller, S. J.; Larson, R. G. *Macromolecules* **1993**, *26*, 1696.

(36) Park, J. O.; Berry, G. C. *Macromolecules* **1989**, *22*, 3022.

(37) Hashimoto, T.; Takebe, T.; Suehiro, S. *Polym. J.* **1986**, *18*, 123.

MA9611679